Bioorganic & Medicinal Chemistry 16 (2008) 6560–6567

Contents lists available at ScienceDirect

Bioorganic & Medicinal Chemistry

journal homepage: www.elsevier.com/locate/bmc

Petrosamine, a potent anticholinesterase pyridoacridine alkaloid from a Thai marine sponge *Petrosia* n. sp.

Veena S. Nukoolkarn [a,d], Suwipa Saen-oon [b], Thanyada Rungrotmongkol [b], Supot Hannongbua [b], Kornkanok Ingkaninan [c,d], Khanit Suwanborirux [d,e,*]

[a] Department of Pharmacognosy, Faculty of Pharmacy, Mahidol University, Bangkok 10400, Thailand
[b] Computational Chemistry Unit Cell, Department of Chemistry, Faculty of Science, Chulalongkorn University, Bangkok 10330, Thailand
[c] Department of Pharmaceutical Chemistry and Pharmacognosy, Faculty of Pharmaceutical Sciences, Naresuan University, Phitsanulok 65000, Thailand
[d] Center for Bioactive Natural Products from Marine Organisms and Endophytic Fungi (BNPME), Bangkok 10330, Thailand
[e] Department of Pharmacognosy, Faculty of Pharmaceutical Sciences, Chulalongkorn University, Bangkok 10330, Thailand

ARTICLE INFO

Article history:
Received 6 February 2008
Revised 7 May 2008
Accepted 9 May 2008
Available online 15 May 2008

Keywords:
Anticholinesterase
Pyridoacridine
Petrosamine
Molecular docking
Petrosamine-*Tc*AChE interaction

ABSTRACT

Two pyridoacridine alkaloids, including a known petrosamine and a new 2-bromoamphimedine were isolated from a Thai marine sponge *Petrosia* n. sp. The alkaloids were characterized on the basis of 1D and 2D NMR, MS, and IR spectroscopy. Only petrosamine showed strong acetylcholinesterase inhibitory activity approximately six times higher than that of the reference galanthamine. A computational docking study of petrosamine with the enzyme from the electric eel *Torpedo californica* (*Tc*AChE) showed the major contribution to the petrosamine-*Tc*AChE interaction to be arising from the quaternary ammonium group of petrosamine.

1. Introduction

Neurodegenerative diseases involving impairment of cognitive functions, such as the dementia of Alzheimer's disease (AD), are the most common health problems in elderly populations. The rationale for the current major therapeutic approach to treating AD is directed to the inhibition of acetylcholinesterase (AChE), based on the hypothesis that this disease results from a defect in the cholinergic system.[1] Thus, AChE inhibitors are the most widely developed compounds for the symptomatic treatment of this disease. Some AChE inhibitors like physostigmine or tarcine are known to have limitations such as short half-life or side effects like hepatotoxicity. Galanthamine, an amaryllidaceous alkaloid obtained from *Leucojum aestivum*, is a long-acting, selective, reversible, and competitive AChE inhibitor. Galanthamine has been clinically used in Europe and the USA[3] and is marketed as a hydrobromide salt under the trade name of Razadyne®, formerly Reminyl®. This drug is known to produce significant improvement of cognitive function in the treatment of AD and to have very low toxicity and side effects.[2] However, to date, all long term studies have shown clinical efficacy to decline with time as a result of either loss of drug efficacy or the relentless progression of the disease. Therefore, the search for novel potent, selective and less side effect AChE inhibitors has been desirable.

In the course of our study for bioactive substances from marine organisms, we have discovered two pentacyclic pyridoacridine alkaloids, namely petrosamine (**1**) and 2-bromoamphimedine (**2**), from a Thai marine sponge *Petrosia* n. sp. Marine invertebrates, especially sponges, have been proven as a rich source of pyridoacridine alkaloids which elaborate highly colored alkaloids based on the 11H pyrido[4,3,2-*mn*]acridine skeleton.[4] Since the discovery of the first pyridoacridine alkaloid, amphimedine,[5] more than 60 related alkaloids have been reported.[6] Many of these alkaloids have generated interests in their synthesis[7] and biological activities, including antifungal activity,[8] anti-HIV activity,[9] cytotoxic activity,[10] and topoisomerase II inhibition through intercalation into DNA.[11] In this context, we describe the anti-AChE activity-guided fractionation, structure elucidation, and AChE inhibitory activity of compounds **1** and **2**. The molecular docking study is focused on predicting the binding modes of **1** and **2** to the AChE from the electric eel *Torpedo californica* (*Tc*AChE).

* Corresponding author. Tel.: +66 2 218 8363; fax: +66 2 254 5195.
E-mail address: skhanit@chula.ac.th (K. Suwanborirux).

0968-0896/$ - see front matter © 2008 Elsevier Ltd. All rights reserved.
doi:10.1016/j.bmc.2008.05.027

2. Results and discussion

2.1. Chemical structures of 1 and 2

In the preliminary examination, the blue crude MeOH extract of a Thai marine sponge, *Petrosia* n. sp. showed a strong inhibitory effect on AChE. The MeOH extract was further partitioned to give the EtOAc, *n*-BuOH, and aqueous extracts. All extracts were evaluated for AChE inhibitory TLC bioassay as described by Rhee et al.[12] Only the *n*-BuOH extract exhibited activity by showing a clear active zone at the blue spot (R_f 0.25; solvent system: organic phase of $CHCl_3$/MeOH/H_2O, 5:10:6). The *n*-BuOH extract was then repeatedly chromatographed on Sephadex LH-20 columns followed by high speed countercurrent chromatography (HSCCC) and silica gel columns to afford petrosamine (**1**, 120 mg, 0.012% yield based on the MeOH extract) and 2-bromoamphimedine (**2**, 3 mg, 0.0003% yield based on the MeOH extract).

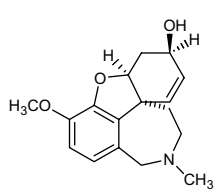

Galanthamine

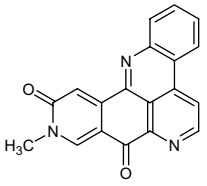

Amphimedine

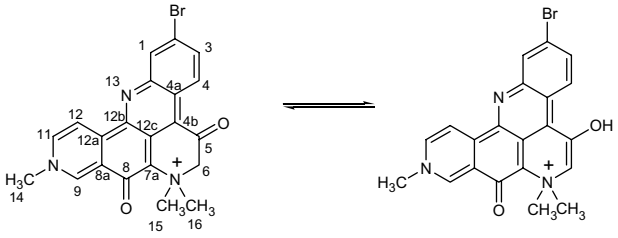

keto-form, 1a enol-form, 1b

[1]

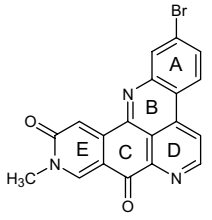

[2]

Compound **1** was obtained as blue needle crystals and identified as the known petrosamine by extensive analyses of spectral data, including 1D and 2D NMR, MS and IR, and comparison with previous reported data.[13] Surprisingly, the ^1H and ^{13}C NMR data of **1** in DMSO-d_6 showed some different signals to the existing reported data. **1** in DMSO-d_6 existed as a keto form showing the methylene signal (C-6) at δ_H 4.75 (2H, s) and δ_C 69.8, while the previous study reported **1** as an enol form showing an olefinic proton signal at δ_H 7.70 (1H, s). To support the above data, **1** in DMSO-d_6 was changed to an enolate form by addition of 100 μmole NaOD and the ^{13}C NMR spectrum was examined. The co-appearance of the olefinic carbon at δ_C 126.5 and the oxygenated olefinic carbon at δ_C 142.0 with the broad methylene carbon at δ_C 69.2 and the carbonyl carbon at δ_C 186.8 suggested the presence of the enolate–keto forms of **1**. However, **1** existed as the enol form in D_2O or CD_3OD.

The structure of **2** was elucidated by interpretation of NMR and MS data and comparison to the NMR data of amphimedine.[5] The TOFMS showed the pseudomolecular ion $[M+H]^+$ and the isotopic peaks at *m/z* 392 and 394 with the ratio 1:1, indicating the presence of one bromine atom in the molecule. The molecular formula of $C_{19}H_{10}N_3O_2Br$ was established by the accurate mass from ESITOFMS showing the $[M+H]^+$ peak at *m/z* 392.0035. The UV spectrum showed maximal absorption at λ_{max} (MeOH) 236, 278, 309, and 371 nm indicating a polyheteroaromatic system. In addition, the absorption band at 1680 cm^{-1} in the IR spectrum and the carbon signal at δ_C 174.7 in the ^{13}C NMR spectrum revealed the presence of an α,β-unsaturated ketone. Furthermore, the amide functionality was readily assigned by the IR absorption at 1640 cm^{-1} and the amide carbonyl carbon at δ_C 164.2 in the ^{13}C NMR spectrum. The NMR data for **2** are summarized in Table 1. The ^1H NMR spectrum in $CDCl_3$ of **2** showed seven aromatic protons and one singlet of *N*-methyl protons. Due to the solubility limitation of **2** in common organic solvents, **2** was dissolved in $CDCl_3$ added with 0.5 mmole TFA-*d* in order to obtain the better *S/N* signals in the ^{13}C NMR spectrum. In addition to the above two carbonyl carbons, the ^{13}C NMR spectrum in $CDCl_3$/TFA-*d* revealed one *N*-methyl carbon, seven aromatic methine carbons, and nine quaternary carbons. Interestingly, the proton signals of H-5 and H-6 appeared as well-defined doublets with J = 5.5 Hz in $CDCl_3$ and these signals became broad singlets and moved downfield in $CDCl_3$/TFA-*d*. Analyses of the ^1H NMR and $^1H,^1H$ COSY spectra in $CDCl_3$ indicated the presence of three spin systems. The first system consisted of three coupled protons [δ_H 8.74 (1H, d, 1.9 Hz, H-1), 8.21 (1H, d, 8.7 Hz, H-4), and 8.04 (1H, dd, 8.7, 1.9 Hz, H-3)] which were assigned to the 1,2,4-trisubstituted aromatic ring (ring A). The second spin system comprised two ortho-coupled protons in a pyridine ring (ring D) with characteristic chemical shifts and coupling constants at δ_H 9.30 (1H, d, 5.5 Hz, H-6) and 8.55 (d, 5.5 Hz, H-5). The third system consisted of three singlet protons of the *N*-methyl at δ_H 3.78 (3H, H_3-14) and two olefinic protons at δ_H 8.78 (1H, H-9), and 8.00 (1H, H-12) in ring E. The adjacency of these partial structures was assured by the HMBC experiment in $CDCl_3$/TFA-*d*. Long-range H-C correlations observed in the HMBC spectrum from H-4 to C-4a and C-4b supported the connection between ring A and ring B. Correlations from H-9 to C-12b and H-12 to C-12b ensured the connection between ring C and ring E. Furthermore, correlations from N-CH_3 protons to C-9 and C-11 confirmed the presence of the amide functionality in ring E. The quaternary aromatic carbon (δ_C 126.2) and the carbonyl carbon (δ_C 174.7) were assigned to the remaining positions at C-7a and C-8, respectively. Interestingly, the non-splitting broad signals of H-5 and H-6 in $CDCl_3$/TFA-*d* showed no correlations in the HMBC spectrum, but the correlation between H-4 to C-5 confirmed the structure of **2**. Thus, **2** was established as a new 2-bromoamphimedine.

2.2. AChE inhibitory activity assay

To investigate the potential inhibitory effects on AChE of **1** and **2**, the *Tc*AChE inhibitory activity of each compound was measured using a microplate reader based on the modified Ellman method.[14] **1** showed the IC_{50} value of 0.091 μM while galanthamine showed the IC_{50} value of 0.590 μM (Fig. 1 and Table 2). The result showed that **1** displayed potent AChE inhibitory activity about six times the potency of the reference galanthamine whereas **2** showed very weak potency with IC_{50} higher than 300 μM. This encouraging result led us to study molecular docking of **1** and **2** in order to assess their probable binding mode in the active site of *Tc*AChE.

Table 1
^{1}H and ^{13}C NMR data for **2**

No.	δ_C (mult)[a]	δ_H (mult, *J*, Hz)[b]	δ_H (mult, *J*, Hz)[c]	HMBC[c]
1	126.9 (d)	8.74 (d, 1.9)	8.84 (d, 1.9)	C-3, C-13a
2	117.9 (s)			
3	138.1 (d)	8.04 (dd, 1.9, 8.7)	8.22 (dd, 1.9, 8.8)	C-1, C-13a
4	133.7 (d)	8.21 (d, 8.7)	8.35 (d, 8.8)	C-4a, C-4b, C-5, C-13a
4a	114.4 (s)			
4b	122.0 (s)			
5	122.7 (d)	8.55 (d, 5.5)	8.95 (br s)	
6	146.0 (d)	9.30 (d, 5.5)	9.43 (br s)	
7a	126.2 (s)			
8	174.7 (s)			
8a	113.4 (s)			
9	145.7 (d)	8.78 (s)	8.90 (s)	C-11, C-12a, C-14
11	164.2 (s)			
12	115.6 (d)	8.00 (s)	8.17 (s)	C-8a, C-9, C-11, C-12a, C-12b
12a	142.8 (s)[d]			
12b	142.8 (s)[d]			
12c	111.1 (s)			
13a	144.9 (s)			
14	39.7 (q)	3.78 (s)	3.80 (s)	C-9, C-11

[a] ^{13}C NMR (125 MHz), $CDCl_3$/TFA-d.
[b] ^{1}H NMR (300 MHz), $CDCl_3$.
[c] ^{1}H NMR (500 MHz), $CDCl_3$/TFA-d.
[d] Overlapping signal.

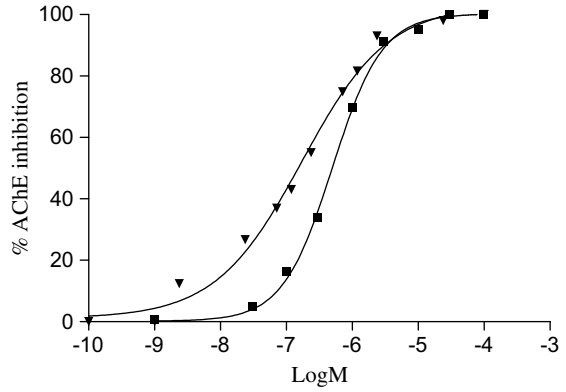

Figure 1. Inhibition effects of **1** (▼) and galanthamine (■) on *Tc*AChE. Percentage inhibitions were assayed by the procedure described in the text. The points are averages of one typical experiment done in triplicate.

Table 2
Estimated free energy of binding and IC_{50} values of the AChE inhibitors

Compound	Estimated free energy of binding (kcal/mol)		IC_{50} [a] (μM)
	1DX6	1EVE	
Galanthamine	−20.58	−18.94	0.590 ± 0.099
1a	−24.94	−24.50	0.091 ± 0.034
1b	−24.56	−23.74	
2	−14.89	−13.69	>300

[a] The IC_{50} values are expressed as mean ± standard deviations ($n = 3$) from individual determinations, each performed in triplicate.

2.3. Molecular docking study

Two different crystal structures (1DX6- and 1EVE-proteins) of acetylcholinesterase (*Tc*AChE), from the electric eel *T. californica*, were used as the target protein in the molecular docking study. These are *Tc*AChEs complexed with galanthamine[15] and donepezil, respectively.[16] The first structure was selected to be the reference target protein while the latter one was used for evaluation of the docking algorithm. If the docking results in terms of ligand's orientations and relative binding energies are similar to each other, this would provide confident quality predictions of the petrosamine and 2-bromoamphimedine binding to *Tc*AChE enzyme.

To verify the method used, molecular docking of the reference compound, galanthamine, was examined. The result showed that the docked conformation of galanthamine reproduced its originally bound conformation in *Tc*AChE gorge[15] of 1DX6-protein with the root-mean-square deviation (rmsd) of 0.83 Å. This indicated the reliability of the docking procedure which was used to predict the binding modes of **1** and **2**. Both forms of petrosamine, a keto-form (**1a**) and an enol-form (**1b**), were taken into consideration refer to the above experimental results which observed two possible tautomers. The docking results for the four systems, galanthamine, **1a**, **1b**, and **2** in the two vicinities of *Tc*AChE (1DX6- and 1EVE-proteins), were compared in term of molecular orientation and estimated free energy of binding as given in Figure 3 and Table 2, respectively. In addition, the amino acid residues located around the active site of *Tc*AChE within the radius of 6 Å from the inhibitor were analyzed and summarized in Table 3.

The obtained docking results for 1DX6 are comparable to those of 1EVE in which the obtained free energies of binding −24.94 kcal/mol (1EVE: −24.50 kcal/mol) of **1a** and −24.56 kcal/mol (1EVE: −23.74 kcal/mol) of **1b** are significantly lower than that of −20.58 kcal/mol (1EVE: −18.94 kcal/mol) of galanthamine. This indicates higher potency of **1** compared to that of galanthamine. The binding free energy of **2** (−14.89 kcal/mol in 1DX6 and −13.69 kcal/mol in 1EVE) is highest in both systems. Taking the above into account, the calculated binding free energies for both systems are in the following order **1a** ≈ **1b** < galanthamine ≪ **2**. This is in good agreement with the experimental IC_{50} shown in Table 2.

Regarding the binding of these compounds to *Tc*AChE given in Table 3, it was shown that almost 25 amino acid residues were observed to locate within 6 Å far from the investigated inhibitors. Note that among the catalytic triad,[17,18] Ser200, His440 and Glu327, only the first two residues were detected within this distance. Although, Glu327 lies longer than 6 Å away from all four inhibitors, it indirectly binds to the inhibitors via the strong hydrogen bond network among the catalytic triad where the hydrogen bond distances are 2.62 Å from Glu327 to His440 and 2.68 Å from His440 to Ser200 (Fig. 2A.1–D.1). This is similar to what found in the second protein, 1EVE, where the first distance of 2.82 Å and

Table 3
Amino acid residues of *Tc*AChE within 6 Å from the inhibitors (marked as **X**)

Protein	Compound	Gln69	Tyr70	Val71	Asp72	**Trp 84**	Asn 85	Pro86	Gly117	Gly118	Gly119	Tyr121	Scr122	Gly123	Ser124	**Glu 199**	**Ser200**	Ala201	Trp233	Phe288	Phe290	**Phe330**	Phe331	Tyr334	**His440**	Gly441
1DX6	Ref.*				x	X			x	x	x	x				X	X	x	x	x	x	X		x	X	x
	1a	x		x	x	X	x	x	x	x			x	x		X	X					X	x	x	X	x
	1b	x		x	x	X	x	x	x	x			x	x		X	X					X	x	x	X	x
	2	x	x	x	x	X	x	x	x	x		x	x	x	x							X	x	x	X	
1EVE	Gal**					X			x	x	x	x				X	X	x	x	x	x	X		x	X	x
	1a	x	x	x	x	X	x	x	x	x	x	x	x	x		X	X					X	x	x	X	x
	1b	x	x	x	x	X	x	x	x	x			x	x		X	X					X	x	x	X	x
	2	x	x	x	x	X	x	x	x	x			x	x	x							X	x	x	X	

* Galanthamine originally obtained from its crystal complex, 1DX6.[14]
(Key amino acids, as shown in Figure 2, are given in bold letter).
** Gal is abbreviated for galanthamine.

second one of 2.76 Å were shown in Figure 2A.2–D.2. These remarkable interactions are direct interactions between the inhibitors and the two catalytic residues, Ser200 and His440. They were observed only for galanthamine, **1a** and **1b** with distances between heavy atoms laying in the range 2.6–3.7 Å (Fig. 2A–C). The lack of these important interactions for **2** (Fig. 2D) could be one of the reasons for its lower *Tc*AChE inhibitory activity in comparison to the other compounds. Additionally, strong interactions to the charge residue of Glu199 were not observed for **2**. The formation of a strong hydrogen bond between galanthamine and Glu199 was observed where the distance of 2.59 Å agrees well with that of 2.70 Å yielded from the X-ray crystallography.[15]

Relative to galanthamine and **2**, the docking data show that both **1a** and **1b** bind stronger and locate closer to the catalytic triad of the binding gorge. Major interaction arises from the quaternary ammonium group at ring D of **1**. Strong electrostatic interaction between N^+ and Glu199 was indicated by the distances between N^+ to O1 and O2 with distances of 4.76 Å (1EVE: 4.88 Å) and 4.14 Å (1EVE: 4.23 Å) for **1a** and 4.79 Å (1EVE: 4.92 Å) and 4.00 Å (1EVE: 4.06 Å) for **1b**, respectively. Note that the O1–N and O2–N distances for **2** were increased by c.a. 2 Å and 1 Å, respectively. This clearly indicates that the quaternary dimethyl ammonium group at ring D of **1** donates the major and strong interactions to the key amino acid residues located on the binding site (Glu199 and Ser200).

Owning to our docking conformation, the obtained Phe330-compound distances, defined in Figure 2A–D, are 4.50 Å (1EVE: 5.27 Å), 3.66 Å (1EVE: 4.12 Å), 3.60 Å (1EVE: 3.95 Å), and 3.76 Å (1EVE: 4.10 Å) for galanthamine, **1a**, **1b** and **2**, respectively. In addition, all compounds had direct π-π interactions between their six-membered ring and Trp84 located above the inhibitor in which two distances were detected in the range of 3.3–4.6 Å.

Summarizing, the binding orientation of the two highly potent compounds, galanthamine and petrosamine (both keto and enol forms) are fundamentally different; galanthamine forms a 'π stack' only with Trp84, whereas the charged amine of petrosamine clearly forms the π–π interactions to both Trp84 and Phe330 as well as interacting through a salt bridge with Glu199. In contrast, the interaction of galanthamine with Glu199 occurs via a hydrogen bond from a hydroxyl group in the ligand. The quoted distances from the quaternary N of petrosamine to Glu199 serves to emphasize the different binding orientation of petrosamine, compared to galanthamine.

In Figure 3, the electrostatic potential surfaces for the above mentioned residues, lying at the catalytic region, were calculated for **1a** and **2**. Both plots show mainly negative (red) regions that fit well to the positive charge substrate such as acetylcholine or the positive charge inhibitors, such as **1**. It is clearly demonstrated by the electrostatic potential surfaces that **1** is more preferable than **2** in term of electrostatic interaction. Moreover, the more tightly binding of **1** to *Tc*AChE in comparison to **2** appears to arise from the lost of number of interactions with the surrounded residues in the 2-bromoamphimedine/enzyme complex shown in Table 3.

3. Conclusions

Two pyridoacridine alkaloids, including a known petrosamine (**1**) and a new 2-bromoamphimedine (**2**) were isolated from a Thai marine sponge, *Petrosia* n. sp. The AChE inhibitory assay revealed **1** to possess an IC_{50} value lower than galanthamine of about six times. The molecular docking study demonstrated that the order of free energy of binding of **1**, **2**, and galanthamine was in good agreement with the IC_{50} values of their anti-AChE activity. The docked conformations gave the explanation and understanding for the binding mode of these compounds to their binding gorge

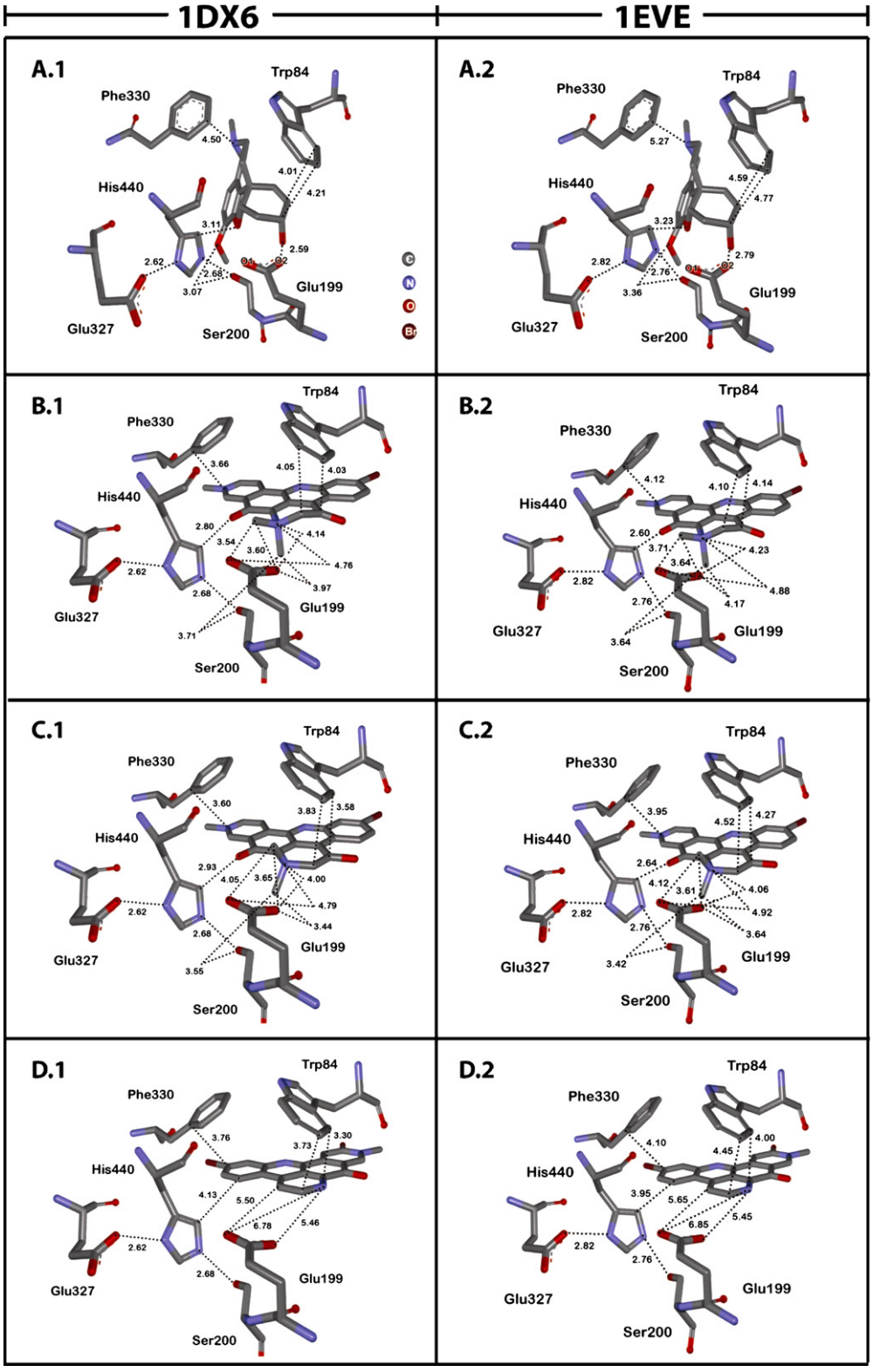

Figure 2. Predicted docking conformations of galanthamine (A), **1a** (B), **1b** (C) and **2** (D) in the catalytic triad binding gorges of *Tc*AChE, 1DX6 and 1EVE.

of *Tc*AChE. One major observation found from computational docking is that the quaternary ammonium group at ring D of **1** donated the major and strong interactions to the key amino acid residues, Trp84, Glu199 and Ser220. Therefore, this study suggests petrosamine as a new potent AChE inhibitor for neurodegenerative diseases.

4. Experimental

4.1. Animal material

The greenish black sponge materials were collected in the intertidal zone of Phuket Island, Thailand in June 2000, frozen on site,

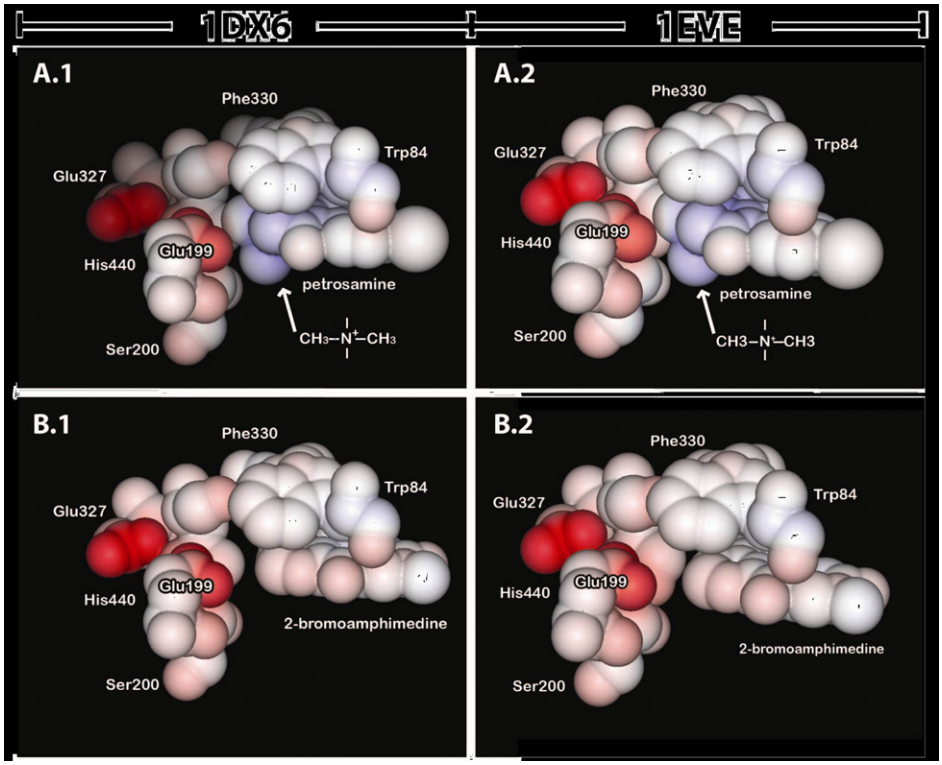

Figure 3. The electrostatic potential surfaces of the amino acid residues located at the catalytic binding gorges of *Tc*AChE, 1DX6 and 1EVE, with the docked bound conformations of **1a** (A) and **2** (B) (negative regions are in red and positive regions are in blue).

and stored at −20 °C before extraction. The sponge was identified as *Petrosia* n. sp. (Class Demospongiae, Order Haplosclerida, Family Petrosiidae) by Dr. John N. A. Hooper of Queensland Museum, South Brisbane, Australia. The voucher specimens of this sponge (PK 00-01) and the underwater photographs are available from our laboratory. A voucher specimen is also deposited at Queensland Museum under the specimen number QM G320225.

4.2. General experimental procedure

The IR spectra were measured on a Perkin-Elmer FT-IR 1760X spectrometer. The UV spectra were obtained from a Shimadzu UV-160A UV/vis spectrophotometer. The ^{1}H and ^{13}C spectra of **1** were recorded at 300 and 75 MHz, respectively, on a Bruker ADVANCE DPX-300 FT-NMR spectrometer. The ^{1}H and ^{13}C spectra of **2** were recorded on a JEOL JMN-A500 NMR spectrometer at 500 and 125 MHz, respectively. The chemical shifts (ppm) of the residual deuterated solvents (δ_H = 7.25, δ_C = 77.0 for $CDCl_3$ and δ_H = 2.49, δ_C = 39.7 for DMSO-d_6) were used as references. Proton detected heteronuclear correlations were measured using HMQC (optimized for $^{1}J_{HC}$ = 145 Hz) and HMBC (optimized for $^{n}J_{HC}$ = 4 and 8 Hz) pulse sequences. The ESITOFMS were measured on a Micromass LCT mass spectrometer, and the lock mass calibration was applied for the determination of an accurate mass.

4.3. Extraction and isolation

Freshly thawed specimens of the sponge (10 kg wet wt) were cut into small pieces and macerated four times with MeOH (8 L, each). The combined extracts were concentrated in vacuo to obtain the MeOH extract which was partitioned between EtOAc and H_2O to obtain the EtOAc extract (2 g) and the aqueous part. The aqueous part was further partitioned with *n*-BuOH to yield the active *n*-BuOH extract (8 g). The *n*-BuOH extract was chromatographed on Sephadex LH-20 columns by eluting with MeOH and followed by HSCCC using the lower organic phase of $CHCl_3$/MeOH/H_2O (5:10:6) to yield 7 fractions. The second fraction was chromatographed on a silica gel column using $CHCl_3$/EtOAc (1:4) as an eluent and repeatedly purified by silica gel columns using the mixture of the lower phase of $CHCl_3$/MeOH/H_2O (5:10:6) and $CHCl_3$ in the ratio 1:8 to yield **2** as a yellow solid (3 mg). The sixth fraction was successively separated on a Sephadex LH-20 column by eluting with MeOH/EtOAc (1:4) to yield a blue compound, **1** (120 mg).

4.3.1. Petrosamine (1)

Dark blue needles: mp > 330 °C; IR (film) 3056, 1644, 1583, 1531, 1494, 1422, 924, 838 cm^{-1}, UV (MeOH) λ_{max} (ε) 286 (36,418), 346 (11,732), 369 (11,183), 414 (6,161) nm; ^{1}H NMR (DMSO-d_6, 300 MHz) δ_H 3.83 (6H, s, H_3-15/H_3-16), 4.60 (3H, s, H_3-14), 4.75 (2H, s, H_2-6), 7.92 (1H, dd, *J* = 2.0, 9.2 Hz, H-3), 8.37 (1H, d, *J* = 2.0 Hz, H-1), 9.16 (1H, d, *J* = 9.2 Hz, H-4), 9.17 (1H, d, *J* = 5.3 Hz, H-11), 9.29 (1H, d, *J* = 5.3 Hz, H-12), 9.88 (1H, s, H-9); ^{13}C NMR (DMSO-d_6, 75 MHz) δ_C 48.3 (q, C-14), 53.1 (q, C-15/C-16), 69.8 (t, C-6), 114.2 (s, C-7a), 114.3 (s, C-12c), 120.0 (s, C-4a), 121.7 (d, C-12), 122.9 (s, C-2), 126.3 (d, C-4), 128.8 (s, C-4b), 131.5 (s, C-12a), 131.8 (d, C-1), 135.1 (d, C-3), 139.9 (s, C-8a), 141.4 (s, C-12b), 142.1 (s, C-13a), 142.5 (d, C-11), 145.6 (d, C-9), 161.3 (s, C-8), 187.2 (s, C-5); HR FABMS *m/z* 422.0505 $[M]^+$ (calcd. for $C_{21}H_{17}O_2N_3Br$ 422.0504).

4.3.2. 1 + NaOD

^{13}C NMR (DMSO-d_6, 75 MHz) d_C 47.8 (q, C-14, **1a** + **1b**), 52.6 (q, C-15/C-16, **1a** + **1b**), 69.2 (t, C-6, **1a**), 113.7 (s, C-7a, **1a** + **1b**), 113.7 (s, C-12c, **1a** + **1b**), 119.6 (s, C-4a, **1a** + **1b**), 121.3 (d, C-12, **1a** + **1b**), 122.5 (s, C-2, **1a** + **1b**), 125.8 (d, C-4, **1a** + **1b**), 126.5 (d, C-6, **1b**), 128.3 (s, C-4b, **1a** + **1b**), 131.0 (s, C-12a, 1a + 1b), 131.4 (d, C-1, **1a** + **1b**), 134.6 (d, C-3, **1a** + **1b**), 139.5 (s, C-8a, **1a** + **1b**), 141.0 (s, C-12b, **1a** + **1b**), 141.7 (s, C-13a, **1a** + **1b**), 142.0 (d, C-5, **1b**), 142.0 (d,

C-11, **1a** + **1b**), 145.1 (d, C-9, **1a** + **1b**), 160.8 (s, C-8, **1a** + **1b**), 186.8 (s, C-5, **1a**).

4.3.3. 2-Bromoamphimedine (2)

A yellow solid: mp > 300 °C; IR (film) 1680, 1640, 1593 cm^{-1}, UV (MeOH) 236 (23,225), 278 (8,680), 309 (8,797), 371 (4,653) nm; ESITOFMS *m*/*z* 392.0035 $[M+H]^+$ (calcd. for $C_{19}H_{11}O_2N_3Br$ 392.0034); ^1H (500 MHz) and ^{13}C (125 MHz) NMR data see Table 1.

4.4. AChE inhibitory activity assay

4.4.1. Chemicals

Acetylthiocholine iodide (ATCI), *Tc*AChE, bovine serum albumin (BSA), 5,5-dithiobis[2-nitrobenzoic acid] (DTNB), and galanthamine were obtained from Sigma (St. Louis, MO). All organic solvents (analytical grade reagent) were purchased from Merck (Darmstadt, Germany). 50 mM Tris–HCl pH 8.0 was used as a buffer throughout the experiment unless otherwise stated. *Tc*AChE used in the assay was from the electric eel, *Torpedo californica* (type VI-S lyophilized powder, 480 U/mg solid, 530 U/mg protein). The lyophilized enzyme was prepared in the buffer to obtain 1130 U/ml stock solution. The enzyme stock solution was kept at −80 °C. The further enzyme-dilution was dissolved in 0.1% BSA in buffer. DTNB was dissolved in the buffer containing 0.1 M NaCl and 0.02 M $MgCl_2$. ATCI was dissolved in deionized water.

4.4.2. TLC assay

The TLC combined with bioassay for AChE inhibitors was modified from the method of Rhee et al.[12] The samples were dissolved and spotted on the silica gel TLC plate. After having developed the TLC plate in the appropiate solvent system, the plate was dried at room temperature and then sprayed with 30 mM ATCI followed by 20 mM DTNB. The plate was dried at room temperature for 45 min and then sprayed with 10.17 U/ml *Tc*AChE. After 20 min, the plate was observed under visible light. The TLC plate appeared as a yellow background with white spots of AChE inhibitory compounds.

4.4.3. Microplate assay

The assay for AChE inhibitory activity was performed according to the methods developed by Ellman et al.[19] and Ingkaninan *et al.*[14] Briefly, 125 μl of 3 mM DTNB, 25 μl of 15 mM ATCI, 50 μl of Tris-buffer, and 25 μl of sample solution were added to the wells followed by 25 μl of 0.28 U/ml *Tc*AChE. The microplate was then read at 405 nm every second for 2 min by a CERES UV 900C microplate reader (Bio-Tek instrument, USA). The velocities of the reactions were measured. Enzyme activity was calculated as a percentage of the velocities of the samples compared to that of the blank. Inhibitory activity was calculated by deducing the percentage of enzyme activity from one hundred percent. Each experiment was done in triplicate. The IC_{50} value, corresponding to the inhibitor concentration that causes 50% inhibitory activity, was determined with the software package Prism (Graph Pad Inc, San Diego, USA) using 8–10 different concentrations of the inhibitors.

4.5. Molecular docking experiment

The molecular docking was carried out to investigate the binding mode using AutoDock version 3.0.[20] Since, galanthamine has been used in the AChE inhibitory assay, the crystal structure of AChE complexed with galanthamine, PDB code: 1DX6,[15] was chosen to represent the enzyme structure in this present work. In addition, the second crystal structure, AChE complexed with donepezil (PDB code: 1EVE),[16] was used for the docking procedure to determine if the same general orientation and relative free energies of inhibitor-enzyme binding were obtained. Initially, galanthamine was taken out from the *Tc*AChE complex and then docked back to its binding gorge of the enzyme to validate the procedure of docking.

For ligand setup, the atomic coordinates of galanthamine were directly obtained from the crystal *Tc*AChE complex (1DX6) and then added up with the hydrogen atoms by taking into account the hybridization of the covalent bonds. The structure of **1** was taken from the NCI database which was subsequently modified to generate the new alkaloid **2**. All ligand geometries were optimized with the HF/3-21G level of theory on the Gaussian98 software package[21] in order to adjust bond lengths and angles involving hydrogen atoms. Atomic charges of ligand were assigned using the Gasteiger–Marsili formalism.[22] The compounds were then setup for docking with the help of AutoTor. In contrast, both polar and non-polar hydrogen atoms were added to the protein. The Kollman all-atom charges and atomic solvation parameters were then assigned.

The grid maps representing the protein were calculated with AutoGrid. The grids (one for each atom type in the ligand, plus one for the electrostatic interactions) were chosen to be sufficiently large to include not only the binding gorge but also significant portions of the surrounding surface. The dimensions of the grid were 60 Å × 60 Å × 60 Å, with a spacing of 0.375 Å between the grid points and the center on the reference compound, galanthamine. The docking search for the orientations of ligand binding to the gorge of *Tc*AChE was carried out using the new empirical free energy function and the Lamarckian genetic algorithm.

Acknowledgments

We gratefully acknowledge financial supports from the Thailand Research Fund through the Royal Golden Jubilee Ph.D. program # PHD/00054/2541 and the New Researcher Grant # MRG4880041. BNPME is supported by a grant for the Center of Excellence, Commission on Higher Education, Thailand. Thanks are due to the Scientific and Technology Research Equipment Center (STREC), and the Pharmaceutical Research Instrument Center of the Faculty of Pharmaceutical Sciences, Chulalongkorn University for providing all research facilities.

References and notes

1. Perry, E. K. *Br. Med. Bull.* **1986**, *42*, 63–69.
2. (a) Maelicke, A.; Samochocki, M.; Jostock, R.; Fehrenbacher, A.; Ludwig, J.; Albuquerque, E. X.; Zerlin, M. *Biol. Psychiatry* **2001**, *49*, 279–288; (b) Thomsen, T.; Kewitz, H. *Life Sci.* **1990**, *46*, 1553–1558.
3. Marco-Contelles, J.; Carreiras, M. D. C.; Rodriguez, C.; Villarroya, M.; Garcia, A. G. *Chem. Rev.* **2006**, *106*, 116–133.
4. Molinski, T. F. *Chem. Rev.* **1993**, *93*, 1825–1838.
5. Schmitz, F. J.; Agarwal, S. K.; Gunnasekera, S. P.; Shoolery, J. N. *J. Am. Chem. Soc.* **1983**, *105*, 4835–4836.
6. (a) Marshall, K. M.; Barrows, L. R. *Nat. Prod. Rep.* **2004**, *21*, 731–751; (b) Skyler, D.; Heathcock, C. H. *J. Nat. Prod.* **2002**, *65*, 1573–1581.
7. (a) Beauchaard, A.; Chabane, H.; Sinbandhit, S.; Guenot, P.; Thiéry, V.; Besson, T. *Tetrahedron* **2006**, *62*, 1895–1903; (b) Delfourne, E.; Kiss, R.; Le Corre, L.; Dujols, F.; Bastide, J.; Collignon, F.; Lesur, B.; Frydman, A.; Darro, F. *Bioorg. Med. Chem.* **2004**, *12*, 3987–3994; (c) Delfourne, E.; Darro, F.; Bontemps-Subielos, N.; Decaestecker, C.; Bastide, J.; Frydman, A.; Kiss, R. *J. Med. Chem.* **2001**, *44*, 3275–3282; (d) Zhang, D.; Llorente, I.; Liebeskind, L. S. *J. Org. Chem.* **1997**, *62*, 4330–4338.
8. McCarthy, P. J.; Pitis, T. P.; Gunawardana, G. P.; Kelly-Borge, M.; Pomponi, S. A. *J. Nat. Prod.* **1992**, *55*, 1664–1668.
9. Taraporewala, I. B.; Cessac, J. W.; Chanh, T. C.; Delgado, A. V.; Schinazi, R. F. *J. Med. Chem.* **1992**, *35*, 2744–2752.
10. (a) Matsumoto, S. S.; Sidford, M. H.; Holden, J. A.; Barrows, L. R.; Copp, B. R. *Tetrahedron Lett.* **2000**, *41*, 1667–1670; (b) Matsumoto, S. S.; Biggs, J.; Copp, B. R.; Holden, J. A.; Barrows, L. R. *Chem. Res. Toxicol.* **2003**, *16*, 113–122; (c) Thale, Z.; Johnson, T.; Tenney, K.; Wenzel, P. J.; Lobkovsky, E.; Clardy, J.; Media, J.; Pietrazkiewicz, H.; Valeriote, F. A.; Crews, P. *J. Org. Chem.* **2002**, *67*, 9384–9391.
11. (a) McDonald, L. A.; Eldredge, G. S.; Barrows, L. R.; Ireland, C. M. *J. Med. Chem.* **1994**, *37*, 3819–3827; (b) Stanslas, J.; Hagan, D. J.; Ellis, M. J.; Turner, C.;

Carmichael, J.; Ward, W.; Hammonds, T. R.; Stevens, M. F. *J. Med. Chem.* **2000**, *43*, 1563–1572; (c) Marshall, K. M.; Matsumoto, S. S.; Holden, J. A.; Concepción, G. P.; Tasdemir, D.; Ireland, C. M.; Barrows, L. R. *Biochem. Pharmacol.* **2003**, *66*, 447–458.
12. Rhee, I. K.; van de Meent, M.; Ingkaninan, K.; Verpoorte, R. *J. Chromatogr. A* **2001**, *915*, 217–223.
13. Molinski, T. F.; Fahy, E.; Faulkner, D. J.; Van Duyne, G. D.; Clardy, J. *J. Org. Chem.* **1988**, *53*, 1340–1341.
14. Ingkaninun, K.; de Best, C. M.; van der Heijden, R.; Hofte, A. J. P.; Karabatak, B.; Irth, H.; Tjaden, U. R.; van der Greef, J.; Verpoorte, R. *J. Chromatogr. A* **2000**, *872*, 61–73.
15. Greenblatt, H. M.; Kryger, G.; Lewis, T.; Silman, I.; Sussman, J. L. *FEBS Lett.* **1999**, *463*, 321–326.
16. Kryger, G.; Silman, I.; Sussman, J. L. *Struct. Fold Des.* **1999**, *7*, 297–307.
17. Pilger, C.; Bartolucci, C.; Lamba, D.; Tropsha, A.; Fels, G. *J. Mol. Graphics Modell.* **2001**, *19*, 288–296.
18. Zaheer-ul-haq; Wellenzohn, B.; Liedl, K. R.; Rode, B. M. *J. Med. Chem.* **2003**, *46*, 5087–5090.
19. Ellman, G. L.; Lourtney, D. K.; Andres, V.; Gmelin, G. *Biochem. Pharmacol.* **1961**, *7*, 88–95.
20. Morris, G. M.; Goodsell, D. S.; Halliday, R. S.; Huey, R.; Hart, W. E.; Belew, R. K.; Olson, A. J. *J. Comput. Chem.* **1998**, *19*, 1639–1662.
21. Frisch, M. J.; Trucks, G. W.; Schlegel, H. B.; Scuseria, G. E.; Robb, M. A.; Cheeseman, J. R.; Zakrzewski, V. G.; Montgomery, J. A.; Stratmann, R. E.; Burant, L. C.; Dapprich, S.; Millam, J. M.; Daniels, A. D.; Kudin, K. N.; Strain, M. C.; Farkas, O.; Tomasi, J.; Barone, V.; Cossi, M.; Cammi, R.; Mennucci, B.; Pomelli, C.; Adamo, C.; Clifford, S.; Ochterski, J.; Petersson, G. A.; Ayala, P. Y.; Cui, Q.; Morokuma, K.; Malick, D. K.; Rabuck, A. D.; Raghavachari, K.; Foresman, J.B.; Cioslowsko, J.; Ortiz, J. V.; Fox, D. J.; Keith, T.; Al-Laham, M. A.; Peng, C. Y.; Nanayakkara, A.; Gonzalez, C.; Challacombe, M.; Gill, P. M. W.; Johnson, B. G.; Chen, W.; Wong, M. W.; Andres, J. L.; Head-Gordon, M.; Replogle, E. S.; Pople, J. A. *Gaussian 98 (Version A.1), Gaussian Inc., Pittsburgh, PA, 1998.*
22. Gasteiger, J.; Marsili, M. *Tetrahedron* **1980**, *36*, 3219–3228.